IOSR Journal of Applied Physics (IOSR-JAP)
e-ISSN: 2278-4861.Volume 8, Issue 4 Ver. IV (Jul. - Aug. 2016), PP 01-11
www.iosrjournals.org

Numerical Simulation And Performance Optimization Of $Cu(In,Ga)Se_2$ Solar Cells

Sampson Oladapo OYEDELE[1,2]*, Bernabé MARÍ SOUCASE[2,], Boko AKA[1]
[1] *Université Nangui Abrogoua, UFR des Sciences Fondamentales et Appliquées (SFA), 02 BP 801 Abidjan 02 (Côte d'Ivoire)*
[2] *Universitat Politècnica de València, Departament de Física Applicada-IDF, Camí de Vera, s/n, 46022 València (SPAIN)*

Abstract: *Numerical simulation has been used to investigate the effect of the different layer components on the performance of $CuInGaSe_2$ solar cells. The effect of the gallium content in the $Cu(In_{1-x}Ga_x)Se_2$ absorber and defect concentration in the $CuInGaSe_2$ absorber and in the CdS buffer layer as well as the effect of defects at the n-CdS/CIGS interface on the cell implementation has been analyzed using SCAPS-1D software. The main photovoltaic parameters of simulated devices: open-circuit voltage (Voc), short-circuit current (Isc), fill factor (FF), and conversion efficiency (η) were analyzed as a function of the defect density in the different layers. According to numerical simulation the highest conversion efficiency for CIGS solar cell is reached when the Ga content (Ga/Ga+In) in the CIGS absorber layer is about 30%. This result is validated by experimental results. When the defect density of CIGS absorber layer increases from de 10^{12} cm^{-3} to 10^{18} cm^{-3}, keeping constant the other parameters, the efficiency decreases by 83%. When the density of defects at the CdS/CIGS interface increases from 10^{12} to 10^{18} cm^2, keeping constant the other parameters, both open circuit voltage and conversion efficiency also decrease but both parameters are less sensitive to interface defects than to absorber defects. This effect is related to recombination, which is more important when it takes place at absorber defects than at interface defects.*

Keyword: *Numerical simulation; CIGS solar cell; SCAPS-1D; defects; efficiency.*

I. Introduction

Polycrystalline $Cu(In_{1-x},Ga_x)Se_2$ is a very promising material for thin film photovoltaic and also highest reported efficiently for a laboratory scale CIGS, solar cell is 22.3% which was gained by Japanese CIGS producer Solar Frontier [1]. This is a first time that CIS has crossed the 22% efficiency boundary a level not yet surpassed by any other thin-film or multi-crystalline silicon technology.

Before that, the $Cu(In_{1-x}Ga_x)Se_2$ (CIGS) based thin film solar cells have earned special interest among the thin film solar cell and there are several important merits in CIGS to reach high efficiency: (i) the band gap of CIGS can be varied from 1.06 to 1.7 eV in such a way by varying Ga composition to obtain required bandgap that meets the solar spectrum to absorb most of the photons, (ii) the thermal expansion coefficient of CIGS matches with soda-lime glass, (iii) in order to make abrupt junction with window layer, the carrier concentration and resistivity of CIGS can be varied by controlling its intrinsic composition without extrinsic doping, (iv) the band gap of absorber layer decides how much quantity of thickness to be needed for the absorber in the thin film solar cell [2].

The CIGS has a direct bandgap with a high optical absorption coefficient which using absorber of only a few microns thick. Furthermore, CIGS thin film exhibits a tunable band gap [3] an excellent outdoor stability and radiation hardness.

The chemical complexity of the layers of a chalcopyrite cell and the presence of a hetero-interface make us understand that the physical phenomena is more difficult than in the case of polycrystalline silicon so we need fundamental studies to a better understanding the physico-chemical of these devices to better control their technology.

Also CIGS solar cells have complex defect structures at their active interfaces. The identification and removal (or passivation) of defects is, therefore, becoming crucial in improving the reproducibility, performance, stability, yield, and lifetime of PV solar cells. This improved understanding of solar cell structures could lead to the achievement of stable, low-cost, and highly efficient solar cells in the future.

Several documents were published on material growth, processing and characterization on one side, and on the performance of finished cells and modules on the other but the interpretation of the experimental data is often difficult due to lack of accurate model and also data about defect, band offsets, carrier density at grain boundaries and interfaces are hard to obtain experimentally.

Therefore numerical modelling to describe PV thin layer devices is a convenient tool to better understand the basic factors limiting the electrical parameters of the cell and to increase their performance.

Numerical modeling of solar cells in thin layers has evolved from a rather exotic research area to a usual practice today.

There were several numerical studies for investigation of thin film solar cells and these reports investigate parameters of cells, which directly contribute in performance of thin film cell [4-9].

Numerical simulations of solar cells have the advantage that all device and material properties are well controlled as they are input parameters of the model and, therefore, evaluation of trends and quantified changes in J-V or QE measurements are possible.

This work aims at using numerical simulations SCAPS-1D [4] to investigate the effect of gallium grading on CIGS cell performance and the effect of defect density in the layers of CIGS and in the interface CdS/CIGS.

Firstly, we will report the modeling and simulation results of CIGS cell with the previously reported experimental result and the agreement between experiment and our simulation is good for the efficiency and validates our set of parameters as a baseline for simulating the influence of the variation of other parameters on the solar cell performances. Secondly we will studies the effect Ga-grading in the absorber CIGS and thirdly we will vary the defect density absorber layer CIGS and the defect at interface CdS/CIGS and we conclude.

II. Methodology

2.1 Cell structure and material parameters

The photovoltaic structure to be studied is based on CIGS absorber with a CdS layer acting as buffer layer and ZnO as window layer. Molybdenum (Mo) was chosen as back contact. Figure 1 shows the sequence of the different layers of the solar cell, Mo/CIGS/CdS/ZnO. Thicknesses of each layer are also indicated in Figure 1.

In order to run numerical simulation calculations the baseline parameters of all the components of the solar cell have to be defined to be used as inputs for SCAPS software. These parameters can be grouped in three sets; physicochemical properties of the layers themselves, density and main characteristics of defects on each layer and characteristics of the interfaces CIGS/CdS and CdS/ZnO.

Table 1.a displays the layers' properties (bandgap energy, electronic affinity, thicknesses, dielectric constant, electron and hole motilities (μ_n and μ_p), effective density of states in the conduction band and in the valence band (N_C and N_V) and concentration of the acceptors and donors (N_A and N_D) for every layer of the photovoltaic device. In the case of the absorber both energy bandgap and electron affinity was varied to meet the real values for $CuIn_{1-x}Ga_xSe_2$ as a function of the gallium content.

Table 1.b displays the characteristics (type of defect, density electron and/or hole capture cross section) for the Gaussian distributed defects states in the layer components of the CIGS solar cell. The density of defects was varied from 10^{14} to 10^{18} cm^2 to evaluate their effect on the performance of the device.

Table 1.c shows the interface properties (density of defects and electron/hole capture cross sections at the interfaces CIGS/CdS and CdS/ZnO, respectively. The density of defects at the interface CIGS/CdS was varied from 10^{14} to 10^{20} cm^{-2}.

All these materials are well known materials and their properties can be easily found in the literature and experimental studies available in references [5-7].

The absorption and optical parameters used in this paper for CIGS, CdS and ZnO layers were taken from references [8-10] respectively.We have not taken in to consideration the influence of the series and shunt resistance in this calculation. The standard solar spectrum AM1.5 was used for analyzing the behavior of CIGS solar cell under illumination and the temperature was set at 300 K.

2.2 Numerical modeling

The output characteristics of CIGS thin film solar cell were numerically simulated through Solar Cell Capacitance Simulator (SCAPS) software [4].We used the latest version of SCAPS version 3.3 03 to evaluate the influence of defects on the properties of the solar cell. SCAPS is a free program developed at the Gent University by M. Burgelman et al. designed for thin film solar cells 1-D modeling and made available to university researchers in the photovoltaic community since 1998. The user enters parameters to define the different materials and interfaces that compose the solar cell . The main limitation of this software simulation tool is that a very good knowledge of the parameters of the materials composing the cell is needed..

SCAPS 1-D solves the basic semiconductor equations that are the Poisson equation, relating the charge to the electrostatic potential F, and the continuity equations for electrons and holes and gives the performance parameters of the cell. SCAPS treats also some tunneling mechanisms. The model implemented for interface transport in SCAPS is thermionic emission. The thermal velocity of the interface transport equals the smallest thermal velocity of the two neighboring layers [11]. For the defect, we use the same definition for interface defects and bulk defects. However, there are only three possible defects and their charge type cannot be multivalent. For recombination in interface states we used for model the Pauwels-Vanhoutte theory [12-13],

which is an extension of the Shockley-Read-Hall theory [14]. Two tunneling processes involving interface transport are also implemented. For each layer, the material properties should be given to software as inputs. Furthermore, the test conditions including the temperature, illumination, bias voltage, etc. should be set before starting the simulation. The transmission and reflection of the back and front contacts should also be set before running the simulation.

III. Results and discussions

We have investigated the effect of Ga content in CIGS, defects in CIGS, CdS and ZnO and interface defects at interface CdS/CIGS. According to the solar cell structure shown in Figure 1 and the material parameters displayed in Table 1 the output of SCAPS software gives the energy band diagram of the CIGS solar cell. Figure 2 shows the energy band diagram of the CIGS-based solar cell to be analyzed.

$CuInSe_2$ and $CuGaSe_2$ are materials with a direct band gap of 1.06 eV and 1.7 eV, respectively. The difference is mainly due to a difference of the minimum of the conduction band (EC). Therefore, the band gap of the quaternary $CuIn_{1-x}Ga_xSe_2$ material can be tuned to the desired value by adjusting the Ga content.

The energy band gap and electron affinity depends on the Ga content in the CIGS layer and it is defined as Ga/(Ga+In) or 'x' ratio in equations (1) and (2). The dependence of the band gap energy (eq. 1) and electron affinity (eq. 2) with the Ga content were taken from reference [15].

$$Eg = 1.06 + 0.39238\ (x) + 0.24762\ (x)^2 \qquad (1)$$

and

$$\chi_e = 4.6 - 1.15667\ (x) + 0.03333\ (x)^2 \qquad (2)$$

The results of energy band gap and electron affinity calculated by these equations were used in Gallium grading effect on cell performance.

3.1. Effect of Ga content on the cell performance

In order to check the effect of Ga content in the absorber and in the PV devices we have compared the main photovoltaic (PV) parameters for both simulated and experimental data. Figure 3 compares the conversion efficiency of two sets of experimental CIGS-cells for manufactured for different Ga-content of the absorber [15, 16] with our simulation. The dependence with the Ga-content in the absorber is similar for both sets of experimental data reaching the optimal performance for a Ga-content about 30%. The efficiency of CIGS solar cells presented by reference 12 is higher than reference 13 but the behavior with the absorber content is similar. Table 2 compare also with x=0.3 the simulation parameters with the experimental data issued from *Solar cell efficiency tables* 2016 [18]. The conversion efficiency for the simulated CIGS cell is quite close to the real device. This produces a realistic basis for all further simulations.

Band gap energy, Eg, and electron affinity, χ_e, were calculated from equations 1 and 2 the output have been used in the simulation of the performance of $CuIn_{1-x}Ga_xSe_2$ solar cells with different amounts of Ga. Table 3 shows the photovoltaic parameters of the CIGS cell for different Ga contents in the absorber layer. When Ga-ratio (x) increases from 0 to 1 the band gap increases from 1.06 eV ($CuInSe_2$) to 1.7 eV ($CuInGaSe_2$).

Electron affinity decreases from 4.60 to 3.47 eV when x ranges from 0 to 1. According to our numerical simulation results the highest conversion efficiency is reached for CIGS absorbers with Ga-content about 30% (x=0.3). When x increases Eg also increases and as a result V_{OC} increases from 0.54 V to 0.820 V due to the higher bandgap of the absorber. However, Jsc decreases from 41.67 to 25.89 mA/cm^2 because part of the solar spectrum is not harvested by the solar cell [19].

For the Ga ratio exceeding 30% (x>0.3), the overall performance of the CIGS solar cells begins to drop down. The concentration of defect varies with the Ga-content in the absorber alloy The responsible mechanisms for the limitation of the performance for the CIGS solar cells with the high Ga contents are explain by that the concentration of defect varies with the Ga-content in the absorber alloy and the trap density increased exponentially above 0.30, negating any expected increase in efficiency due to the increased band gap concentration of defect by that the concentration of defect varies with the Ga-content in the absorber alloy and the trap density increased exponentially above 0.30, negating any expected increase in efficiency due to the increased band gap [20].

Figure 4 shows the main photovoltaic parameters for the CIGS solar cells as a function of the gallium content. As can be seen the short-circuit current is constant up to Ga contents about 30% and then decreases due to the rise of the bandgap of the CIGS absorber. The open-circuit voltage tends to increase with the amount of Ga but its slope reduces for Ga content higher than 40%. As a result, both fill factor and efficiency increases with the Ga content, reaching a maximum about 30% of Ga and the decreasing with higher Ga contents.

3.2 Effect of defects density of layers

A large variety of crystal defects determine the electronic properties of semiconductors. Some of these act as donors or acceptors that are essential for the operation of a solar cell as they produce the p-n junction.

Others are recombination centers that limits the lifetime of minority carries and hence the efficiency of these cells. Still others are responsible for carrier scattering or recombination; some of them trap carriers and influence the space charge that determines the carrier transport. A better knowledge of the diversity of these defects helps to improve their performance. One distinguishes:

- point defects, such as single atoms or vacancies in an otherwise near-ideal lattice;
- line defects (dislocations);
- surface defects relating to external or internal crystal surfaces; and
- volume defects, relating to small, three-dimensional inclusions or defect associates.

Defects formation energies in the prototype chalcopyrite $CuInSe_2$ semiconductor were obtained through *ab initio* methods by S.B. Zhang [21]. These results were validated by experimental measurements using various techniques. Table 4 shows the formation energies and types of defects in $CuInSe_2$ according to references [21] and [22].

To better understand the effects of defects on CIGS solar cells, the photovoltaic parameters for CIGS solar cells have been studied as a function of the defect density in the different layers of the PV device. In this simulation the analysis has taken out by varying the defect density of one layer while keeping the defect density other layers constant. Henceforth we will use the band gap and electron affinity values calculated for CIGS absorbers with x=0.3. Defect densities were varied from 10^{15} cm^{-3} to 10^{19} cm^{-3}.

3.2.1 Effect of defects density of window layer ZnO

In order to study the effect of defects in ZnO we will calculate the photovoltaic parameters for a defects density ranging from 10^{15} to 10^{19} cm^{-3}, while keeping constant the defect densities of both CIGS absorber layer and CdS buffer layer.

Figure 5 displays the main photovoltaic parameters Voc, Jsc, FF and η as a function of the defect density in the ZnO windows layer. From 10^{15} to 10^{18} cm^{-3} defect density, Jsc, η and Voc remain the same and the variation of FF is less than 3% from 10^{18} to 10^{19} cm^{-3}. From 10^{18} to 10^{19} cm^{-3}, Jsc decreases from 36 to 32 mA/cm^2 therefore a decrease of 11 %. Therefore, according to these results the rise of defects density in the ZnO layer has little impact in the performance parameters.

3.2.2 Effect of defects density of buffer layer CdS

In order to study the influence of defect density in the buffer layer in the performance of CIGS-based PV devices, the PV parametres were calculated as a function of an increasing defect density in the CdS buffer layer ranging from 10^{15} to 10^{19} cm^{-3} while keeping constant the defect of absorber CIGS layer and window ZnO layer.

Figure 6 shows the main photovoltaic parameters Voc, Jsc, FF and η as a function of the defect density in the CdS buffer layer. From 10^{15} to 10^{18} cm^{-3} defect density, η drops from 25.87 to 25.70, therefore a decrease of 1%. From 10^{15} to 10^{17} cm^{-3}, J_{sc} drops from 48.17 to 48.13 mA/cm^2 therefore a decrease of 1% and from 10^{17} to 10^{18} cm^{-3}, J_{sc} increases less than 1%. From 10^{15} to 10^{16} cm^{-3}, Voc increases about 2% and from 10^{16} to 10^{18} cm^{-3} it decreases about 3%.

A little variation of photovoltaic parameters is observed for the defect density range studied. The cell performance is quite insensitive to the presence of defects in both buffer and window layers and concentration of defects as high as 10^{19} cm^{-3} produces a fall in the efficiency lower than 1%.

3.2.3 Effect of defects density of absorber layer CIGS.

We varied the defect of layer CIGS from 10^{15} to 10^{19} cm^{-3} while keeping constant the defect of buffer layer CdS and window layer ZnO.

Figure 7 shows the effect of defect density of layer CIGS on cell performance of cell parameters and show that basic parameters were severely affected when we increased the defect 10^{15} to 10^{19} cm^{-3}.

Table 5 shows the performance parameters of the CIGS cell based on different values of defect of layer CIGS. The open-circuit voltage and short-circuit current are degraded by increasing the defect density. Voc drops from 0.758 to 0.417 Volt therefore a decrease of 45%. J_{sc} drops from 43.16 to 22.29 mA/cm^2 therefore a decrease of 48%. Voc decreases less that J_{sc} by the recombination with the localized energy levels, which is created by defects, which cause current leakage. As a result, the conversion efficiency drops from 25.87 to 4.50% therefore a decrease of 83%.

Figure 8 shows the External Quantum Efficiency (EQE) as function of wavelength for different values of defect density in layer CIGS. When the wavelength is in the range of 400-1200 nm, the absorption efficiency quickly decreases with increase of p-CIGS defect.

For a defect density of 10^{15} cm^{-3} the quantum efficiency has a maximum absorption value close to 92% and the device has a moderate ultraviolet response and a strong visible light and red response. The loss in the

ultraviolet part of the incident spectrum can be justified by considering the moderate carrier collection in the n-type layer.

When the defect density increases from 10^{15} cm^{-3} to 10^{19} cm^{-3} the EQE decreases. The low absorption in highest p-CIGS defect is considered that the corresponding spectrum is not completely absorbed by the p-type absorption layer. Higher defect density in p-layer leads to pronounced decrease in the performance parameter of CIGS cell solar than the defects in other layers such CdS and ZnO.

This is justified by the fact that the front layers n-CdS and n-ZnO are always thinner and have lesser absorption than the absorber p-CIGS layer. The bandgap Eg of p-CIGS absorber is equal about to 1.2 eV and the defect have a Gaussian distribution in energy with a width 0.2 eV around the maximum located at 0.6 eV .So we have these defects located near the middle of the gap and thereby act as recombination centers and also the increased density makes the recombination phenomena more significant and causes fewer carriers and subsequently decreasing performance conversion.

3.3 Effect of defects at interface CdS/CIGS

To understand the effect of defects at the interface CdS/CIGS, we increase the defect in interface CdS/CIGS from 10^{15} cm^2 to 10^{20} cm^2 at AM 1.5 conditions (100mW/cm^2) .

Figure 9 shows the variation of cell parameter as function of defect interface CdS/CIGS. In this case all photovoltaic parameters decrease with increasing the defect density in the absorber. In the studied defect range Voc drops from 0.7247 V to 0.5630 V therefore a decrease of 22%. J_{sc} is less sensitive to defects than Voc and only drops 3% (from 41.16 to 39.97 mA/cm^2). The fill factor drops about 5% (from 74.43 to 70.40%). The fall of Voc, Jsc and FF parameters with the defect density results in a drastic reduction of the conversion efficiency from 22.14 to 13.85%, which means a decrease of 37%. However, from 10^{15} to 10^{16} cm^2 the effect is less that from 10^{16} to 10^{19} cm^2, where the defect has influence on the performance of the cell. Therefore, the defects at the CdS/CIGS interface have a minor effect on the performance of CIGS solar cell than the defects density at CIGS absorber layer and this result is in good agreement with Heath et al. [23].

The defects at the CdS/CIGS interface deteriorated the performance parameters of the CIGS cell however these effects are minor than the defects in p-CIGS layer. The recombination at the CdS/CIGS interface is less than at CIGS absorber because a major role in the suppression of interface recombination is played by the Cu-poor surface defect layer that forms in Cu-poor chalcopyrite. XPS studies show the presence of an In-rich n-type material at the surface of the p-type CIGS and causes large band bending that contributes to the device performance [24].

IV. Conclusion

This work has used the capabilities of computer simulation of SCAPS-1D to address the issues of defect in CIGS. The device parameters chosen for the simulation generate the main PV parameters that closely resembles that of the parameters obtain experimentally.

The simulation shows that the highest efficiency for CIGS solar cells is reached when the Ga content in the $CuIn_{1-x}Ga_xSe_2$ absorber (x) is 0.3. Then we have theoretically performed device modeling for an ideal thin film solar cell based on the $CuIn_{0.7}Ga_{0.3}Se_2$ absorber to investigate the effects of defect density in CIGS and defect in interface CdS/CIGS. The main PV parameters such as open circuit voltage, short-circuit current, fill factor and photo conversion efficiency for different types and concentration of defect states were simulated.

The main results are: the defect states in the absorber layer CIGS always deteriorated the performance of CIGS solar cells than defect in interface CdS/CIGS but however for better understanding of these effects we must considered the effects of temperature and thickness. For future improvement of solar cell CIGS the issue of defects should be taken into account.

Acknowledgements

The authors are grateful to Prof Marc Burgelman and colleagues at the University of Gent for providing the SCAPS-1D software reported in this document. One author (O.S.) is grateful to the Applied Physics Department of Universitat Politècnica de València (SPAIN) for hosting him.

References

[1]. http://www.PV-magazine.com (accessed 15.05 16 at 11h36 A.M.)
[2]. K. Subbar Ramaiah, Cu(In, Ga)Se_2 Based Thin Film solar cell, Thin Films and Nanostructures, 35 (2011) 558.
[3]. E.Dilena, Y. Xie, R. Brescia, M. Prato, L. Maserati, R.Krahne, A. Paolella, G. Bertoni, M. Povia, I. Moreels, L. Manna, $CuIn_xGa_{1-x}S_2$,Nanocrystals with Tunable Composition and Band Gap Synthesized via a Phosphine-Free and Scalable Procedure. Chem. Mater. 25 (2013) 3180−3187.
[4]. M. Burgelman, P. Nollet and S. Degrave, Modelling polycrystalline semiconductor solar cells, Thin Solid Films 361-362 (2000) 527-53.
[5]. M. Mostefaoui, H. Mazari, S.Khelifi, A. Bouraiou, R. Dabou. Simulation of High Efficiency CIGS solar cells with SCAPS-1D software, Energy Procedia 74 (2015) 736-744.

[6]. H. Ullah, Simulation Studies of Thin Film Photovoltaic Devices, Dissertation for PhD Polytechnic University of Valencia (UPV), Spain Feb 2015.
[7]. J. Song, S.S. Li, C.H. Huang, O.D. Crisalle and T.J. Anderson, Device modeling and simulation of the performance of $Cu(In_{1-x},Ga_x)Se_2$ solar cells, Solid State Electronics, 48 (2004) 73–79.
[8]. P.D. Paulson, R.W. Birkmire, W.N. Shafarman, Optical characterization of $CuIn_{1-x}Ga_xSe_2$ alloy thin films by spectroscopic ellipsometry, J. Appl. Phys.94 (2003) 879-888.
[9]. S. Adachi, Optical constants of crystalline and amorphous semiconductors". Ed. Springer. 1999, pp. 502-506.
[10]. S. Adachi, Optical constants of crystalline and amorphous semiconductors. Ed. Springer. 1999, pp.426-428.
[11]. M. Topič, F. Smole and J. Furlan,Band-gap engineering in CdS/Cu(In,Ga)Se_2 solar cells, J.Appl. Phys, 79 (1996) 8537–8540.
[12]. M. Burgelman, J. Verschraegen, S. Degrave, P. Nollet. Modeling thin film PV devices, Prog. Photovolt. Res. Appl. 12 (2004) 143-153.
[13]. A. Mcevoy, T. Markvart, L.Castaiñer,Practical handbook of Photovoltaics, Fundamentals and Applications. Elsevier Ltd. (2012) pp 323-371.
[14]. M. Burgelman, K. Decock, S. Khelifi, A. Abass, Advanced electrical stimulation of thin film solar cells, Thin Solid Films 535 (2013) 296–301.
[15]. N. Khoshsirat, N. Amziah, M. Yunus, M. Nizar Hamidon, S. Shafie, Analysis of absorber layer properties effect on CIGS solar cell performance using SCAPS, Optik 125 (2015) 681-686.
[16]. S. Samaneh, K. Sayyed-Hossein, Model for increased efficiency of CIGS solar cells by a stepped distribution of carrier density and Ga in the absorber layer, Sci. China-Phys Mech Astrom , 56 (2013) 1533-1541
[17]. J. Malmstrom, J. Wennerberg, M. Bodegard, L. Stolt, 17th European Photovoltaic Solar Energy Conference, Munich (2001) 1265.
[18]. M.A. Green, Solar cell efficiency tables (version 47), Research and Applications 24, (2016) 807
[19]. H. Jasenek, U. Rau, H.W. Schock, Influence of the Ga-content on the bulk defect densities of Cu In,Ga Se_2 , Thin Solid Film 387 (2001) 71-73.
[20]. T. Walter, R. Menner, M. Ruckh, L, K. Schock, Parameter studies and analysis of high efficiency $Cu(In,Ga)Se_2$ based solar cells, Proc 22nd IEEE PVSC Conf, (1991) 924-929.
[21]. S.B. Zhang, S. Wei, A. Zunger, H. Katayama-Yoshida, Defect physics of the $CuInSe_2$ chalcopyrite semiconductor, Phys. Rev. B57 (1998) 9642-9646
[22]. G. Dagan, F. Abou-Elfotouh, D. J. Dunlavy, R. J. Matson, and D. Cahen, Chem. Mater. **2**, (1990.) 286-293
[23]. J. T. Heath, J. D. Cohen, W. N. Shafarman, Bulk and metastable defects in CuIn1-xGaxSe_2 thin films using drive-level capacitance profiling, J. Appl. Phys. 95 (2004),1000
[24]. A. Bouloufa, K. Djessas, A. Zegadi, Numerical simulation of $CuIn_xGa_{1-x}Se_2$ solar cells by AMPS-1D. Thin Solid Films 515 (2007) 62-85.

Highlights

- Photovoltaic performance of CIGS solar cells were obtained as function of Ga content.
- Defects in the buffer and window layers have low influence on solar cell performance.
- Defects at the interface can reduce the efficiency of solar cell up to 30%.
- Defects in absorber layerare very important and are able to cancel out the efficiency.

TABLES

Table 1.a. Layer parameters for the different layers of a CIGS-based solar cell at 300 K.

Parameter	Units	p-CIGS	n-CdS	n-ZnO
Eg (Band gap)	eV	Varied from 1.06 to 1.7	2.42	3.3
χ_e(Electron affinity)	eV	Varied from 3.47 to 4.60	4.4	4.2
w (Thickness)	nm	2500	50	150
ε_r (Permittivity)		13.6	10	9
μ_n (electron mobility)	cm^2/Vs	100	100	100
μ_p (holemobility)	cm^2/Vs	25	25	25
N_C (Effective density of states in the conduction band)	cm^{-3}	1.2×10^{18}	1.2×10^{18}	2.2×10^{18}
N_V(Effective density of states in the valence band)	cm^{-3}	1.8×10^{19}	1.8×10^{19}	1.8×10^{19}
N_A (Carrier density of the acceptor)	cm^{-3}	2.0×10^{17}	0	0
N_D (Carrier density of the donor)	cm^{-3}	0	2.1×10^{17}	2.0×10^{19}

Table 1.b. Parameters for the Gaussian distributed defect states in the different layers of a CIGS solar cell.

	Units	p-CIGS	n-CdS	n-ZnO
Type		Donor	Acceptor	Donor
Density of defects	cm^{-3}	Varied from 10^{15} to10^{20}	Varied from 10^{15} to10^{18}	Varied from 10^{14} to10^{18}
Electron capture crosssection (σ_n)	cm^2	9×10^{-13}	1×10^{-17}	1×10^{-12}
Holecapturecrosssection (σ_p)	cm^2	1×10^{-15}	1×10^{-13}	5×10^{-15}
Energy	eV	mid-gap	mid-gap	mid-gap

Table 1.c. Interface properties in CIGS solar cells.

	Interface	CIGS/CdS	CdS/ZnO
Parameter	Type	Donor	Acceptor
Density of defects	cm^{-2}	Varied from 10^{14} to 10^{20}	1×10^{10}
electron capture crosssection (σ_n)	cm^{-2}	1×10^{-13}	1×10^{-15}
hole capture crosssection (σ_p)	cm^{-2}	1×10^{-15}	1×10^{-13}

Table 2. Simulation and experiment parameters of a CIGS cell.

	V_{OC}(V)	J_{sc}(mA/cm^2)	FF (%)	η (%)
Simulation	0.690	41.41	81.2	22.6
Experiment [14]	0.746	36.59	79.3	21.7

Table .3 Simulative performance parameters of the CIGS cell based on different Gacontents in the absorber layerin p-CIGS/CdS/ZnO solar cells.

x=Ga/In+Ga	Eg (eV)	χ_e(eV)	V_{OC}(V)	J_{sc}(mA/cm^2)	FF (%)	η (%)
0	1.060	4.60	0.546	41.67	70.43	16.03
0.31	1.207	4.24	0.690	41.41	81.18	22.63
0.45	1.287	4.08	0.769	35.39	68.27	17.84
0.66	1.422	3.85	0.773	29.37	54.58	16.37
1	1.700	3.47	0.820	25.89	53.87	11.08

Table 4. Formation energy and type of intrinsic defect

Intrinsic defect	Formation energy (eV)	Defect type
In_{Cu} (In antisite, In atom on Cu site)	1.4	donor
Cu_{In} (Cu antisite, Cu atom on In site)	1.5	acceptor
V_{Se} (Se vacancy)	2.4	donor-acceptor
V_{Cu} (Cu vacancy)	2.6	acceptor
V_{In}(In vacancy)	2.8	acceptor
Cu_i (Cu interstitial)	4.4	donor
In_{Se} (In antisite, In atom on Se site)	5.0	donor
Se_{In} (Se antisite, Se atom on In site)	5.5	acceptor
Cu_{Se} (Cu antisite,Cu atom on Se site)	7.5	acceptor
Se_{Cu} (Se antisite, Se atom Cu on Cu site)	7.5	donor
In_i (In interstitial)	9.1	donor
Se_i (Se interstitial)	22.4	acceptor

Table 5. Performance parameters of the CIGS cell based on different values of defect of layer CIGS

Defects density (CIGS)(cm^2)	V_{OC}(v)	J_{sc}(mA/cm^2)	FF (%)	η (%)
10^{15}	0.7583	43.16	79.05	25.87
10^{16}	0.7305	40.89	72.15	21.55
10^{17}	0.6624	36.04	61.91	14.78
10^{18}	0.5337	29.93	55.32	8.84
10^{19}	0.4171	22.29	48.42	4.50

Table 6. Performance parameters of the CIGS cell based on different values of defect interface CdS/CIGS

Interface defects concentration (CdS/CIGS)(cm^2)	V_{OC}(v)	J_{sc}(mA/cm^2)	FF (%)	η (%)
10^{14}	0.7247	41.16	74.43	22.14
10^{15}	0.7227	41.05	73.46	21.86
10^{16}	0.7212	40.89	72.15	21.55
10^{17}	0.7205	40.70	71.97	2113
10^{18}	0.6791	40.49	71.50	19.66
10^{19}	0.6220	40.25	71.01	17.79
10^{20}	0.5630	39.97	70.40	13.85

n-ZnO (150 nm)
n-CdS (50 nm)
p-CIGS (2500 nm)
Mo (500 nm)
GLASS

Figure 1. Schematic diagram of simulated CIGS solar cell indicating the thickness of each layer.

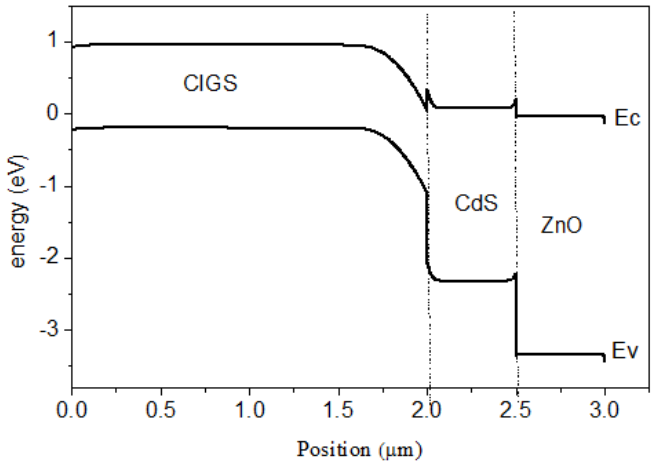

Figure 2. Energy band diagram of a CIGS solar cell.

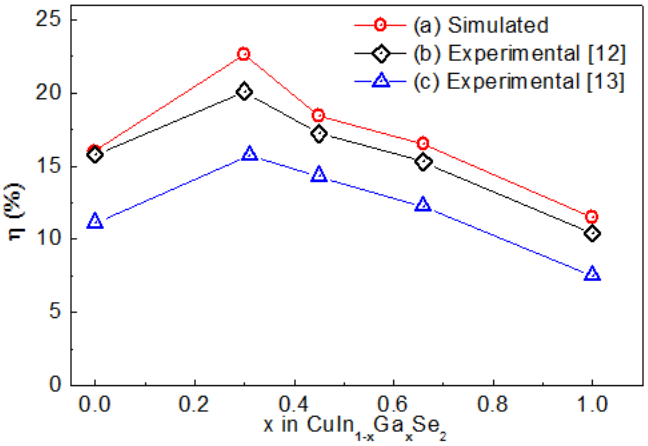

Figure 3: Comparison between the efficiency of a p-CIGSsolar cell as a function of Ga content. (a) simulated by SCAPS, (b and c) from experimental data.

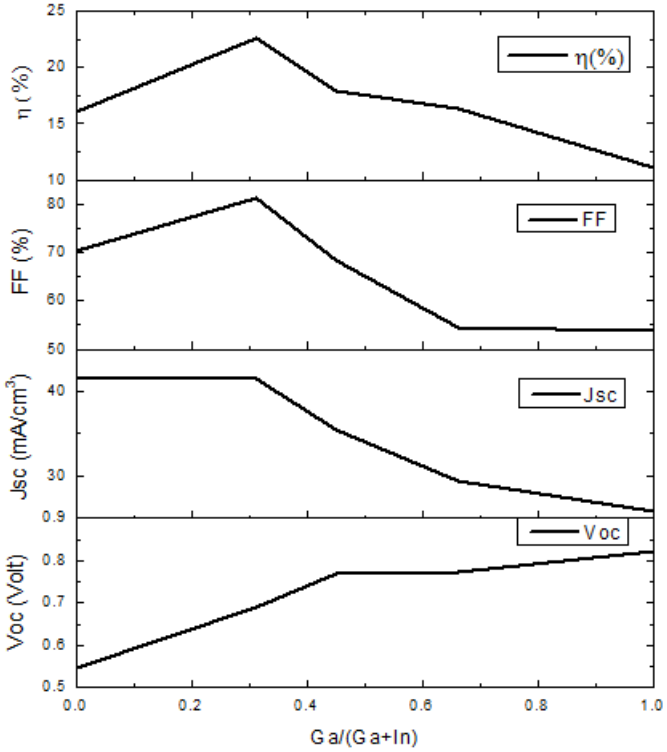

Figure4. Variation of cell parameters as a function of Ga content.

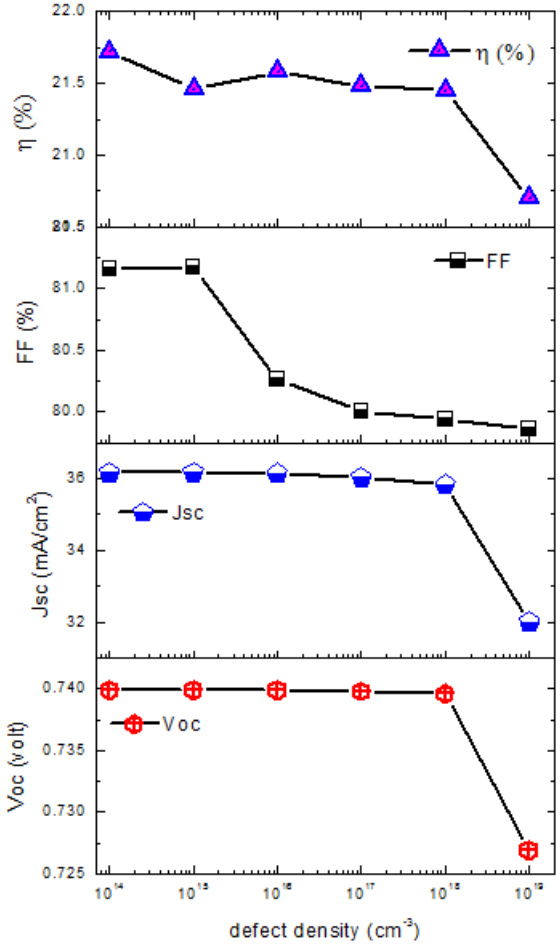

Figure 5. Variation of cell parameters as a function of defects density at ZnO window layer.

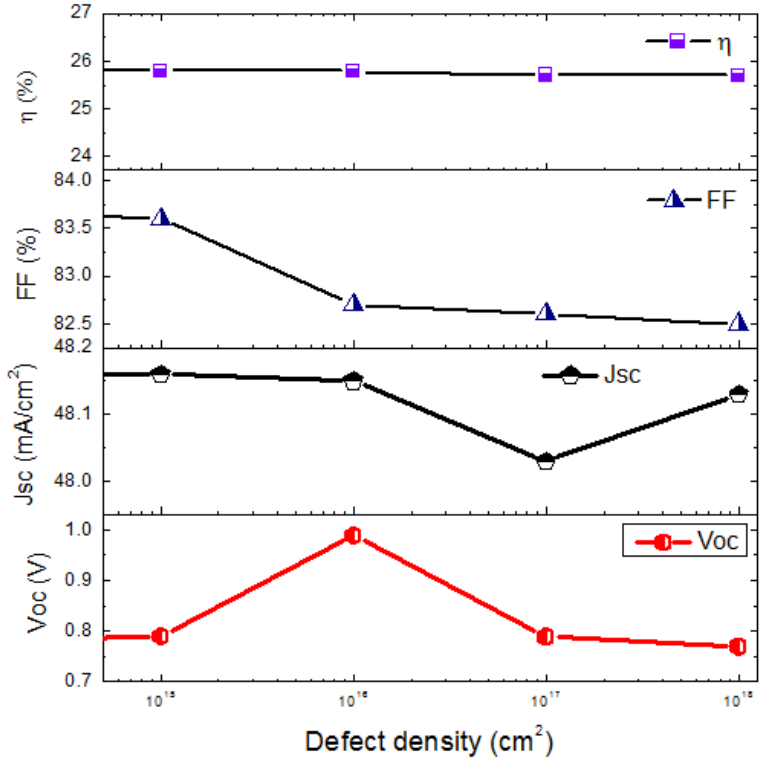

Figure6. Variation of cell parameters asa function of defects density at CdS buffer layer.

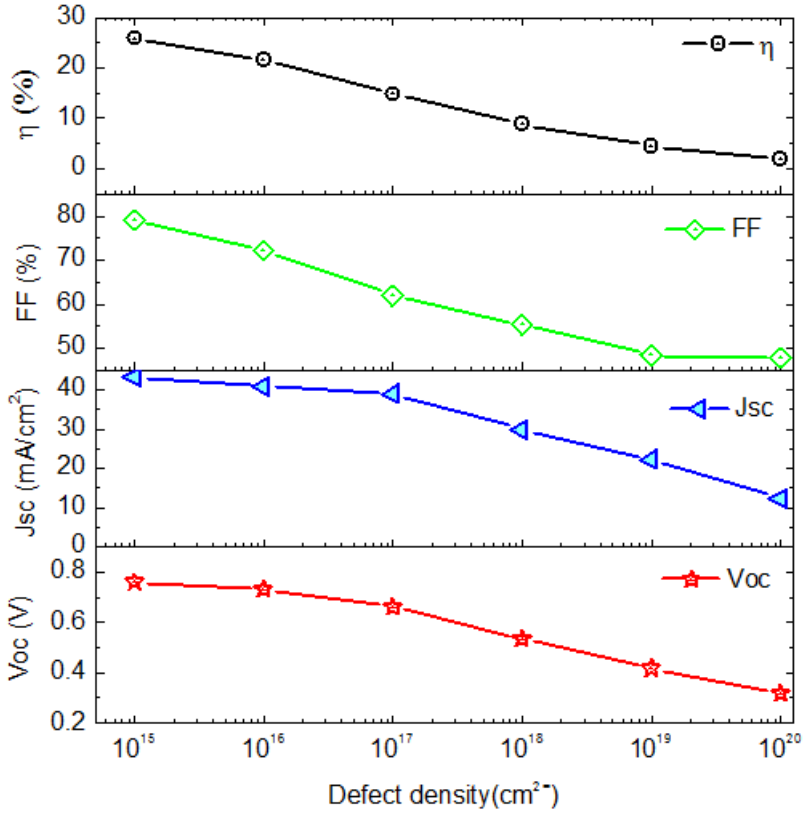

Figure 7. Variation of cell parameter as function of defects density at CIGS absorber layer.

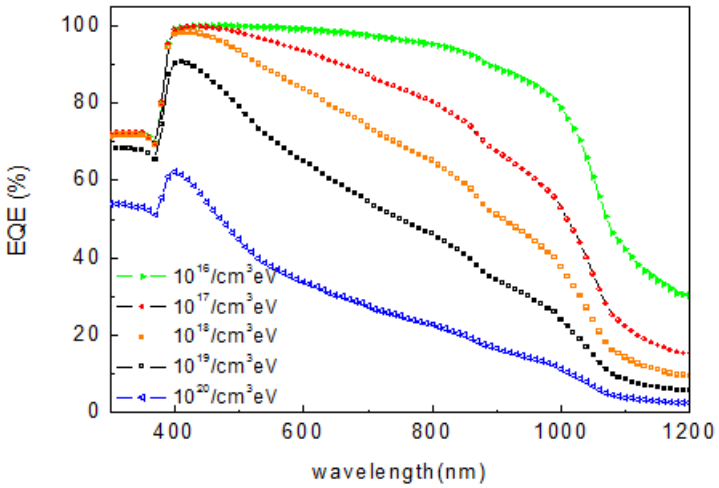

Figure 8.EQE as function of wavelength for different values of defects density at CIGS absorber layer.

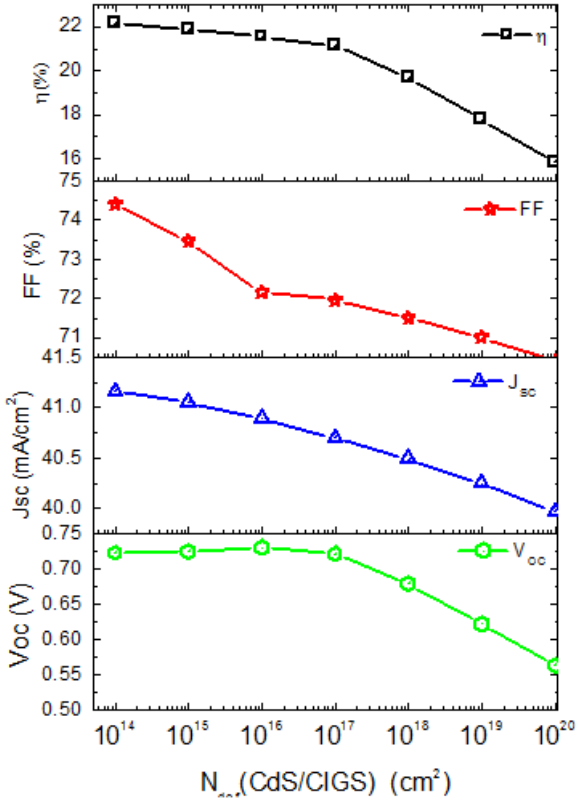

Figure 9.Variation of cell parameter as function of defect density at CdS/CIGS interface.